Available online at www.sciencedirect.com

ScienceDirect

Procedia CIRP 31 (2015) 209 – 214

www.elsevier.com/locate/procedia

15th CIRP Conference on Modelling of Machining Operations

CFD simulation of the Abrasive Flow Machining process

E. Uhlmann[a,b], C. Schmiedel[a,]*, J. Wendler[a]

[a]*Institute for Production Systems and Design Technology (IPK), Pascalstr. 8-9, 10587 Berlin, Germany*
[b]*Technical University Berlin, Institute for Machine Tools and Factory Management (IWF), Pascalstr. 8-9, 10 587 Berlin, Germany*

* Corresponding author. Tel.: +49-030-39006-267; fax: +49-030-391-1037. *E-mail address:* christian.schmiedel@ipk.fraunhofer.de .

Abstract

For the Abrasive Flow Machining (AFM) process, a highly viscous polymeric carrier mixed with abrasive grain is used for deburring, edge rounding and the general improvement of surface quality of workpieces with complex geometries. At present, time-consuming and expensive feasibility studies and parameter analyses are required for each new application. According to a market study of 2012, more than 50 % of AFM users request the availability of a process simulation to model and optimize the flow and predict the results by use of numerical methods. The key challenge is the accurate description of the complex behavior of the viscoelastic abrasive medium. This paper examines a CFD approach to the flow simulation by integrating the non-Newtonian, shear-thinning characteristics of a Maxwell fluid into the inelastic Navier-Stokes equations. With the implementation of the viscoelastic material model in ANSYS CFX, physically reasonable results can be achieved and validated by experimental machining results of additively manufactured SLM workpieces. The results for flat, reference workpieces as well as for turbine blades are discussed and compared to experimental results.

Peer-review under responsibility of the International Scientific Committee of the "15th Conference on Modelling of Machining Operations

Keywords: Abrasive Flow Machining; Viscoelasticity; Simulation; Selective Laser Melting; Additive Manufacturing

1. Introduction

Abrasive Flow Machining (AFM) is a surface and edge finishing process appropriate for complex and internal geometries that are difficult to reach with conventional finishing methods. Another advantage is the high potential for substitution of manual surface finishing [1]. The important components of the AFM process are the machine and the abrasive media as the tool. The latter can be designed individually according to the workpiece properties and consists of a polymeric carrier mixed with abrasive grains (e.g. silicon carbide, boron carbide and diamond). The media is pressed through the workpiece passages by alternating hydraulic cylinders, causing material removal in dependency of the local shear rates. The optimization of the process requires extensive, time and cost consuming tests with various process parameters, such as the machining temperature, the flow velocity and the number of machining cycles [2,3]. In order to reduce the costs and take different geometries of the flow channel into account, FEM [4] and CFD [5,6] simulations can be implemented. To include the complex material behavior of the abrasive media consisting of polymeric carrier and abrasive grains, an accurate material model is required. This is the major challenge due to viscoelastic effects and high particle mass fractions.

In the scope of this paper, AFM is applied on additively manufactured workpieces with typically surfaces of very high roughness. Selective Laser Melting (SLM) is a rapid method to create complex geometries with mechanical properties that are comparable to those of conventionally manufactured ones, but with an insufficient surface quality. CFD Simulations including the application of the material model as introduced by UHLMANN [7] are carried out for generic flat reference workpieces as well as for the workpiece fixture of a turbine blade. The simulation data is compared to experimental machining results. With the use of calculated flow characteristics and machined workpieces, material removal mechanisms are investigated.

Peer-review under responsibility of the International Scientific Committee of the "15th Conference on Modelling of Machining Operations
doi:10.1016/j.procir.2015.03.091

2. AFM processing

In AFM, two hydraulic pistons extrude the abrasive media back and forth through the workpiece passages as shown in Fig.1. During the process, a holding device fixes the workpiece and keeps the abrasive suspension in the flow channel. Firstly, the medium is knead and preheated to the intended machining temperature. After the preparation of the medium, the lower cylinder and workpiece holding device have to be gaplessly filled with the medium. The holding device and the workpiece are clamped between the upper and lower cylinder (Fig.1- I) with a clamping pressure of up to 200 bar. As the pistons move alternating, the medium flows along the surface of the workpiece removing material (Fig.1- II and III). This process is repeated until the desired surface roughness is reached. The process parameters can be entered via a touch-control panel.

Important parameters influencing the machining results are the number of processing cycles, the piston pressure and velocity as well as the medium temperature and composition, including the texture of the carrier, the amount of grain and the size of the abrasive particles. The medium is preheated, because the molecular chains of the polymeric structure need to be stretched to bind the abrasive particles. Preheating can also help to effectively remove air bubbles in the medium. During the process, the temperature has to be maintained at a constant value to assess the corresponding results. Common machining temperatures range between 25 °C and 40 °C.

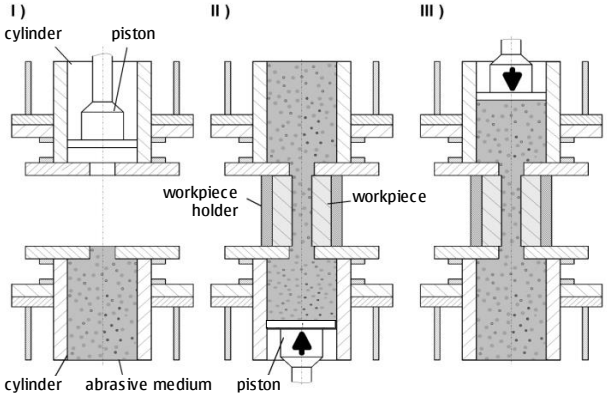

Fig. 1 Setup of AFM process

3. Material modelling

3.1. Measurements

The experimental tests are carried out with AFM media from MICRO TECHNICA TECHNOLOGIES, Kornwestheim, Germany. The polymeric viscoelastic carriers are called MF5 and MF10. The grain material is silicon carbide (SiC) in different grain sizes. To characterize the complex material behavior of these abrasive media, dynamic oscillatory measurements of the complex shear modulus

$$G^* = G' + iG'' \tag{1}$$

are performed with a rotational plate/plate rheometer.

The real part G' of the complex shear modulus is called the storage modulus and represents the elastic characteristics of a material. The imaginary part G'' is called the loss modulus and is a measure of the dissipative properties. The measurement curves of both moduli in dependence on the oscillation frequency ω can also be converted into a complex shear viscosity η^*. Both quantities are connected by formula

$$\eta^* = \frac{G^*}{\omega} = \frac{G'}{\omega} + i\frac{G''}{\omega}. \tag{2}$$

3.2. Maxwell model

In the Maxwell model [8], the rheological properties of a viscoelastic fluid are represented by a purely elastic spring with stiffness G and a purely viscous damping element with damping factor η in series. This combination is called a Maxwell element and represents a certain polymer fraction in the material with its characteristic relaxation time

$$\lambda = \frac{\eta}{G}. \tag{3}$$

Broad molar mass distributions can be represented by the Generalized Maxwell model with several Maxwell elements connected in parallel as shown in Fig. 2. G_0 is the finite, steady state shear modulus for quasi-static deformation.

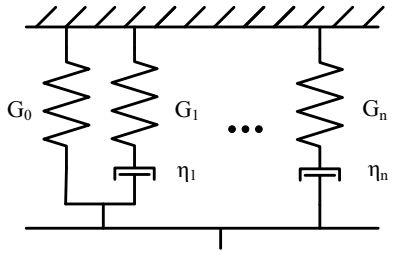

Fig. 2 Generalized Maxwell model

The oscillatory measurement data of the abrasive medium is modelled by three Maxwell elements, what implies seven parameters (G_0, G_1, G_2, G_3, η_1, η_2 and η_3) with an accuracy of more than 99% [7]. For the CFD simulations, continuous model functions for storage and loss modulus are calculated from the Maxwell moduli and relaxation times as described below [8]:

$$G'(\omega) = G_0 + \sum_{k=1}^{3} G_k \frac{(\omega\lambda_k)^2}{1+(\omega\lambda_k)^2} \tag{4}$$

$$G''(\omega) = \sum_{k=1}^{3} G_k \frac{\omega\lambda_k}{1+(\omega\lambda_k)^2}. \tag{5}$$

3.3. Cox-Merz Rule

The Cox-Merz Rule [9] is an empirical relationship supposing that the magnitude of the complex dynamic viscosity from oscillatory measurements and the shear viscosity from steady state measurements are the same for equal values of oscillation frequency ω and shear strain rate $\dot{\gamma}$:

$$\left|\eta^*(\omega)\right| = \sqrt{\eta'(\omega)^2 + \eta''(\omega)^2} = \eta(\dot{\gamma})\big|_{\dot{\gamma}=\omega} . \quad (6)$$

Hence steady state viscosity information can be obtained from oscillatory measurements and vice versa. The rule is applicable for most polymer solutions and melts but it fails for dispersions and gels. It is valid for Maxwell fluids like the abrasive media where mechanical interactions prevail over physical and chemical interactions in the polymer system [8].

Fig. 3 shows the measured viscosity data and the corresponding Maxwell model function for the medium MF10-80S(100) at 25 °C. This medium has a high viscosity and contains a mass fraction of 50 % of SiC grains with an average size of 185 µm. For the CFD simulations, the shear strain rate dependent Maxwell viscosity function has been extended by a lower and upper limit corresponding to the zero and infinite shear viscosity in accordance with the actual material behavior. Minimum and maximum values of the viscosity are also necessary for numerical reasons.

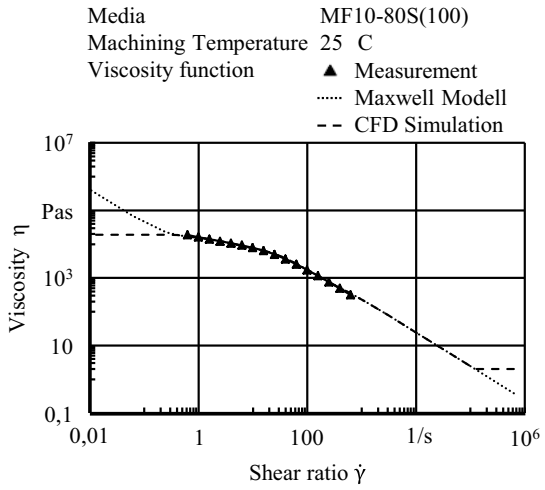

Fig. 3 Measured and modelled viscosity

4. CFD Simulation

4.1. Governing equations

The CFD simulation software ANSYS CFX v15 is based on the inelastic Navier-Stokes equations consisting of the momentum equations

$$\frac{Du_i}{Dt} = \frac{\partial u_i}{\partial t} + u_j \frac{\partial u_i}{\partial x_j} = -\frac{1}{\rho}\frac{\partial p}{\partial x_i} + \frac{1}{\rho}\frac{\partial \tau_{ij}}{\partial x_j} + q_i \quad (7)$$

for the velocity field and the continuity equation

$$\frac{\partial \rho}{\partial t} + \frac{\partial (\rho u_i)}{\partial x_i} = 0 \quad (8)$$

for the pressure field. The transport equations above are solved iteratively by the finite volume technique.

4.2. Geometry

Thorough parameter studies have been carried out for flat reference workpieces to examine the effects of piston velocity, working temperature, polymeric carrier viscosity and processing duration on surface roughness and material removal rate (MRR). The workpiece fixture consists of a rectangular gap containing the sample as one of its walls. The simulation of this simple geometry helps to get a first general impression of the flow characteristics during the AFM process.

Furthermore, the finishing process of a more complex geometry, a turbine blade produced by SLM is simulated to give an example of practically relevant applications. Fig. 4 shows the workpieces and the holding devices.

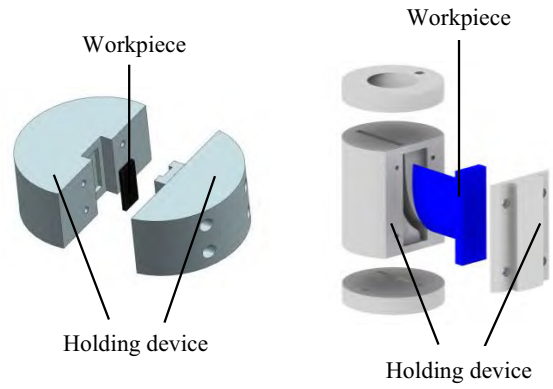

Fig. 4 CAD Model of workpiece and holding device for reference workpiece (left) and turbine blade (right)

In Fig. 5 the computational fluid domains are presented for both workpieces. Convergence studies show that mathematical stable results can be achieved with 4 million elements for the flat reference workpiece and 4.3 million elements for the turbine blade.

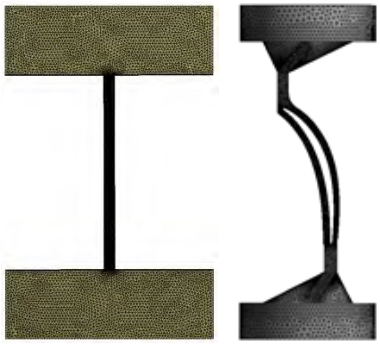

Fig. 5 Computational domain for reference workpiece (left) and blade (right)

4.3. Setup

Isotherm, laminar, steady-state analyses are implemented to model the constant maximal speed of the piston, which takes the main part of a single machining cycle and causing material removal. The fluid is incompressible and non-Newtonian with a variable, shear-thinning viscosity function based on the oscillatory measurements, the Maxwell model and the Cox-Merz rule.

The flow boundary conditions are set with reference to the abrasive flow machine: the velocity at the inlet equals the piston velocity and the pressure at the outlet corresponds to measurements of the static medium pressure during the process. A study of different flow conditions confirmed, that this setup delivers adequate and reasonable results that are comparable to those of a moving wall boundary condition representing the piston at the inlet.

4.4. Wall treatment

Wall slip is known to occur in polymeric fluids [10] and has therefore been observed in the context of the AFM process [5,6]. Thus, the relative movement between the abrasive medium and the workpiece is responsible for the material removal and can be considered as a measure of the machining results. To capture the real fluid behavior at walls, a slip model is marineeded. The CFD simulations are carried out with full and finite slip as well as without slip to examine its effect on the flow.

The following model for finite slip is available in ANSYS CFX v15:

$$u_w = u_S \left(\frac{\tau - \tau_c}{\tau_n} \right) . \quad (9)$$

The applied slip model is a variation of Navier's linear slip law where the wall slip velocity u_w depends on the local value of the shear stress τ and slip occurs only when a critical shear stress τ_c is exceeded.

5. Results and Discussion

5.1. Experimental and numerical results

Material removal is not simulated as this would lead to much more complex CFD simulations due to the geometry changes. The shear strain rate is chosen for comparison between CFD simulation results and the reference workpiece, since the material behavior and grain anchoring is share rate dependent.

Fig. 6 shows the computed shear strain rates at the workpiece wall and the optically measured surface of the reference workpiece after three machining cycles with the medium MF10-24S(100). Obviously, the material removal rate increases locally at the center as well as at the in- and outflow area of the alternating flow of the abrasive medium. The dark areas on the left and the right edge are a result of the clamping of the workpiece. A comparison between the machined and simulated results shows significant correlation between the calculated shear strain rates and the surface quality of the machined workpiece. A local increase of the shear rate leads to a higher storage modulus G' and a decreasing viscosity which corresponds to solid behavior of the viscoelastic carrier. The related firm fixture of the abrasive grains causes the observed intensified material removal in these areas.

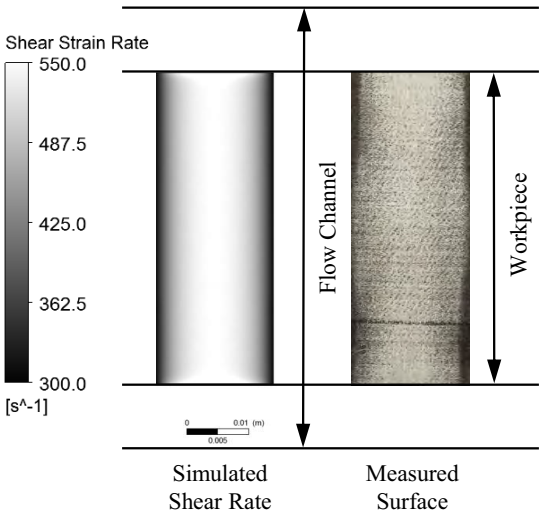

Fig. 6 Simulated shear strain rate (left) and optically measured surface quality (right) on the reference workpiece surface

Similar local differences in surface quality can also be observed for the turbine blade as illustrated in Fig. 7. The process of 10 cycles with MF10-80S(200) results in an even but slow improvement of its surface quality. On the edges, the material removal and roughness reduction are much higher as shown on the right side of Fig. 7.

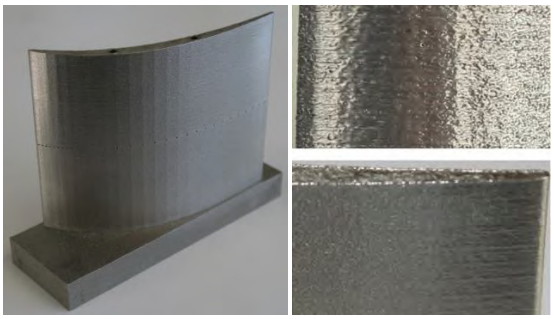

Fig. 7 Machining results for the AM turbine blade

5.2. Shear rate and viscosity

The post-processing of the simulation data gives some general insight into flow and material removal mechanisms during the abrasive flow machining process. The local viscosity is not a constant but dependent on the local shear rate which is a function of the flow velocity gradient. Because of the shear-thinning behavior of the polymeric abrasive media, abrupt velocity changes result in high shear rates and low viscosity. Consequently, viscous properties become less significant whereas elasticity dominates. The abrasive grain is firmly anchored in the stiffened polymer.

Fig. 8 presents the difference between storage and loss modulus on the surface of the simulated flat reference probe. Viscous and elastic properties are balanced for equal values of the storage and loss modulus, i.e. $\Delta G = G' - G''$. Negative values of ΔG represent hence fluid and positive ones solid material behavior. The former occurs in the flow channel corners where the material removal rate is much lower. The latter dominates on the workpiece surface, especially in its center, and causes the described machining results.

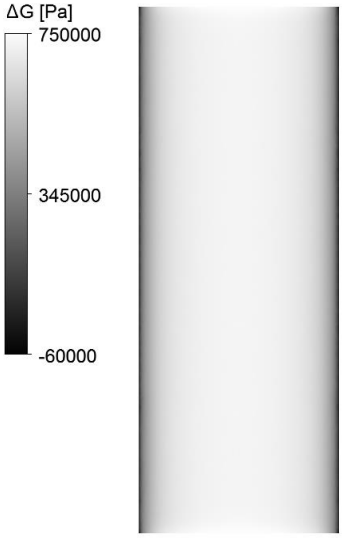

Fig. 8 Calculated storage and loss modulus on the flat reference workpiece

5.3. Pressure drop and velocity distribution

Medium pressure measurements at the in- and outlet of the abrasive flow machine have been carried out during the working cycle. The pressure drop in the flow channel can thus be compared to the simulation results.

It turns out that the simulated pressure drop is strongly dependent on the wall boundary condition. It is comparable to the measured data using a slip-free condition and increases as a function of the boundary layer profile. Consequently, profound investigations of the velocity profile and the real velocity of the medium at the wall are necessary.

Furthermore, a direct connection between the machining results and the measured difference of pressure between inlet and outlet during the process was detected. The material removal rate increases distinctly with the observed pressure drop. The dependence is a result of the varying friction caused losses on the workpiece surface. This observation is very useful as it allows a specific, process-related real-time adjustment of machining parameters.

Fig. 9 illustrates the simulated velocity of the abrasive medium at the wall with the finite slip model as described above. It is a measure for the material removal rate and correlates with the observed experimental results. Due to the critical stress limit, only partial slip occurs in areas with high shear rates and shear stress.

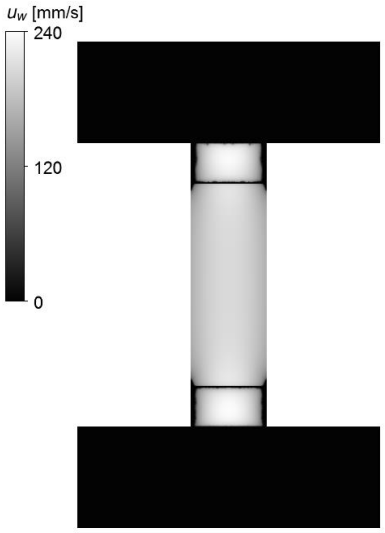

Fig. 9 Simulated wall slip velocity on the flat reference workpiece

The simulated streamlines in the workpiece fixture for the processing of the SLM turbine blade are shown in Fig. 10. During a machining cycle, the leading and trailing edge alternate with the general flow direction. As the blade forces the abrasive medium to separate, high velocity gradients and shear rates occur at both edges resulting in solid-like behavior and a good anchoring of the grains, hence a high material removal rate. This correlates with the described experimental observations as well.

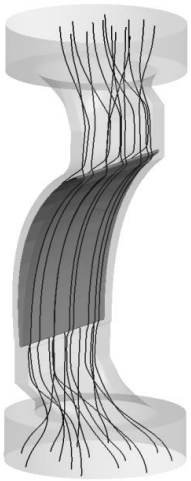

Fig. 9 Simulated streamlines of the abrasive medium in the computational domain of the SLM turbine blade

5.4. Design recommendations

Based on CFD simulations, design criteria for the optimization of workpiece fixtures can be derived. As a consequence, flow related problems can be identified and eliminated during the run-up of experimental tests to reduce the overall time effort for new machining setups.

The goal of surface finishing is a constant high surface quality. The observed, significant edge rounding and inflow area effects are neither detrimental nor necessary. They are a natural flow phenomenon and thus cannot be avoided. A homogenization can be achieved by replacing abrupt cross section changes with smooth transitions. For the flat reference workpieces, funnel-shaped in- and outflow areas would lead to a smoother increase of shear strain rate and uniform machining results. In the same manner, critical sections such as steps and a narrowing in the blade inflow area have been identified in the turbine blade fixture.

6. Conclusion and Outlook

The Maxwell model [7] has been applied to the rheological, oscillatory measurement data of several abrasive media. In the applied, generalized Maxwell material model, 7 parameters consisting of relaxation moduli and relaxation times represent the different polymer fractions.

Based on the Cox-Merz rule, a shear rate dependent viscosity function is obtained and integrated into the commercial CFD simulation software ANSYS CFX v15. Flow simulations of the AFM process have been carried out by solving the steady-state, inelastic Navier-Stokes equations.

The considered machining setups are flat, generic SLM samples that have been the specimen of an experimental parameter study. As a practically relevant complex workpiece, an SLM turbine blade has been used.

The geometry, setup, initial and boundary conditions are widely in accordance with measurements from an abrasive flow machine. Hence, simulation data and machining results can be compared and correlate in terms of local material removal rates and roughness reduction. The simulated pressure drop highly depends on the wall boundary condition. That varies from no slip to finite and slip-free as the former result in very high pressure differences. More investigations and comparison to experimental results are necessary to calibrate the wall boundary condition in further simulations.

One focus of upcoming simulations will be the improvement of the abrasive media flow guidance in the workpiece fixture. This includes the design and optimization of fixtures for emerging and existing applications.

Moreover, the simulation itself can be improved. The wall slip model has to be calibrated based on measured process data such as wall slip velocities using optical access. The elastic properties of the polymeric carrier are of importance as well. The elastically stored energy is recovered, for example when the medium exits a gap. This causes phenomena like extrudate swell and the Weissenberg effect that cannot be neglected in the flow simulation of viscoelastic media.

For this study, variables like the shear rate, complex shear modulus and pressure drop has been used to compare the current simulation data to measurements. A more explicit relation between the experimental and machining results needs to be developed in the form of an empirical material removal model to predict specific local surface quality.

References

[1] BOTTKE; D.: Strömungsschleifen in der industriellen Anwendung (1997). – Industrie Diamanten Rundschau, Band 31, Heft 4, S.346-353.
[2] SZULCZYNSKI, H.: Verfahrensgrundlagen und Technologie des Hubschleifens mit viskosen Schleifmedien (Dissertation). Berlin, 2006.
[3] MIHOTOVIC, V.: Modellbasierte Prozessauslegung des Druckfließläppens am Beispiel keramischer Werkstoffe (Dissertation). Berlin, 2011.
[4] JAIN, R.K.; JAIN, V.K.: Finite element simulation of abrasive flow machining. – Proceedings of the Institution of Mechanical Engineers, Vol. 217, 2003, Part B: Journal of Engineering Manufacture, pp. 1723–1736.
[5] SCHMITT, J.; DIEBELS, S.: Simulation of the abrasive flow machining process. http://onlinelibrary.wiley.com/doi/10.1002/zamm.201200111/pdf. Zeitschrift für Angewandte Mathematik und Mechanik, Vol. 93, 2013, pp. 147–153.
[6] WAN, S.; ANG, Y.J.; SATO, T.; LIM, G.C.: Process modeling and CFD simulation of two-way abrasive flow machining. The International Journal of Advanced Manufacturing Technology, Vol. 71, 2014, pp. 1077–1086.
[7] UHLMANN, E., DOITS, M., SCHMIEDEL, C.: "Development of a material model for viscoelastic abrasive medium in Abrasive Flow Machining". Proceedings of 14th CIRP Conference on Modeling of Machining Operations, 2013.
[8] MEZGER, T.G.: Das Rheologie Handbuch: Für Anwender von Rotations- und Oszillationsrheometern - 4. Auflage. Vincentz Network GmbH & Company KG, Hannover, 2012.
[9] AL-HADITHI, T.S.R. ; BARNES, H.A. ; WALTERS, K.: The relationship between the linear (oscillatory) and nonlinear (steady-state) flow properties of a series of polymer and colloidal systems. – Colloid and Polymer Science, Vol. 270, No. 1,1992, pp. 40–46.
[10] TANNER, R.I.: Engineering Rheology. Oxford University Press, 2000.
[11] CHHABRA, R.P. ; RICHARDSON, J.F.: Non-Newtonian Flow and Applied Rheology: Engineering Applications. Elsevier Science, 2008.
[12] FERRAS, L.L. ; NOBREGA, J.M. ; PINHO, F.T.: Analytical solutions for Newtonian and inelastic non-Newtonian flows with wall slip. http://paginas.fe.up.pt/~fpinho/pdfs/JNNFM2012-slip_GNF.pdf. – Journal of Non-Newtonian Fluid Mechanics,Vol. 175–176, 2012, pp. 76–8.